*Optica Applicata, Vol. XXX, No. 1, 2000*

# Study of laser-produced plasma by means of ion diagnostics at the IPPLM, Warsaw

JERZY WOŁOWSKI

Institute of Plasma Physics and Laser Microfusion, P.O. Box 49, ul. Hery 23, 00–908 Warszawa, Poland.

This paper presents the experimental investigations and analysis of the phenomena in the high-Z plasma produced by a high power nanosecond laser beam with power density up to $10^{15}$ W/cm$^2$. These studies were directed towards determination of collisional and anomalous processes occurring in such plasma as wll as optimization of ion emission from the plasma for possible applications of the laser ion sources.

## 1. Introduction

Investigation of high-Z plasma produced by a high-power laser is interesting for many reasons: 1) in such plasma the laser beam energy is partly converted to X-rays energy used for indirect laser fusion and in laser-plasma X-ray sources applied for various purposes; 2) in high-Z plasma transport of radiation energy is substantial, influencing energetic transformations in this plasma; 3) such plasma is non-ideal in some regions (Coulomb coupling energy is considerable in relation to kinetic energy of particles; 4) high-Z laser plasma can be used as a source of heavy ions for particle accelerators, for ion implantation *etc.*

In this work, we present an application of corpuscular diagnostics to investigation of physical properties of high-Z plasma and measurement of parameters of ion emission from this plasma, important for development of heavy-ion sources. Investigations of laser plasma of various Z by ion-diagnostic methods have been carried out at the Institute of Plasma Physics and Laser Microfusion (IPPLM) for several years (*e.g.*, [1]–[3]). The complementary experiments were also performed with the use of iodine laser system at the Institute of Physics ASCR in Prague, the corpuscular diagnostics came from the IPPLM (*e.g.*, [4]–[6]).

## 2. Characteristic of the physical phenomena occurring in laser-produced plasma

The laser radiation is absorbed mainly in the vicinity of the critical surface due to either the classical absorption (inverse Bremsstrahlung) or a non-classical absorption (resonant absorption, parametric instabilities).

The classical absorption of the laser energy causes the electron temperature to increase strongly and the energy transferred from electrons to ions occurs due to the Coulomb electron-ion interactions. Intense ionization and recombination processes proceed simultaneously. During an expansion of the laser-produced plasma into the vacuum, most of the energy of electrons and ions is transformed into kinetic energy. However, in the process of interaction of laser beam with high-Z targets, more than 50% of the absorbed energy may be reemitted by the hot plasma as X-ray radiation. A part of the X-ray radiation is once again absorbed in the target outside the laser focus where it creates a dense, but colder plasma. Generally, thermal and slow groups of ions are emitted as a result of interaction of the laser radiation with medium- and high-Z targets [2]. In the case of high-power laser interactions ($I\lambda^2 > 10^{15} \cdot \mathrm{Wcm}^{-2}\mu\mathrm{m}^2$), as a result of the non-classical absorption, hot (supra-thermal) electrons are produced; the appearance of the fast group of ions is ascribed just to their existence. Such electrons are usually not desirable, because finally the temperature of plasma decreases.

The hot electron population is formed in the laser plasma by several mechanisms converting the transverse wave of the heating laser beam in longitudinal electrostatic plasma waves, which, in turn, accelerate the electrons by the mechanism of Landau damping.

There are several non-collisional phenomena which occur in laser-plasma interactions. The most obvious one is the spatial inhomogeneity of the laser beam present in our experiments. The hot spots in the beam profile may lead to the onset of filamentation with the adverse consequences for absorption efficiency due to a critical surface ripple. Another reason may be the density profile steeping by the ponderomotive force near the critical surface, which likely occurs when working with a short intense pulse, and the ensuing reflection of a large part of the incident laser power by the density jump. The filamentation alone cannot be responsible for the origin of the hot electrons, whose temperature can be inferred from our experimental data on fast ions.

Under conditions of the experiments performed, the non-collisional absorption connected with parametric instabilities and with ion fluctuations in plasma, should be of particular importance. The ion fluctuations occur as a result of ion-acoustic instabilities concomitant with hot-electron transport in laser plasma. The most likely mechanism accelerating the electrons in our case are parametric instabilities which generate strong electrostatic waves near the critical surface in the plasma.

Following the formula given in [7] on the assumption that the fast ions appear as a result of ion acceleration in the electrostatic potential being created by hot electrons, the temperature of the latter can be estimated as follows:

$$T_{e,h} \approx \frac{\bar{E}_f}{1.25\,\bar{z}_f} \tag{1}$$

where $\bar{E}_f$ and $\bar{z}_f$ are the mean energy and the mean charge state of fast ions, respectively, $T_{e,h}$ is the hot electron temperature.

## 3. Experimental arrangement

The investigations presented in this paper were performed in two experimental systems at the IPPLM, in Warsaw, both equipped with their own Nd:glass laser of comparable laser pulse parameters: the laser energy $E_L \leqslant 15$ J, a pulse duration $\tau_L = 1$ ns and the power density $I_L = 10^{13}-10^{14}$ Wcm$^{-2}$ [8]. The laser beam was focused onto the target by a *f*/2 aspherical lens or by means of an aspherical lens-ellipsoidal mirror illumination system. The target chamber was evacuated to the pressure of about $5\cdot10^{-6}$ torr. Schematic diagrams of the typical experimental arrangements are presented in Figs. 1 and 2.

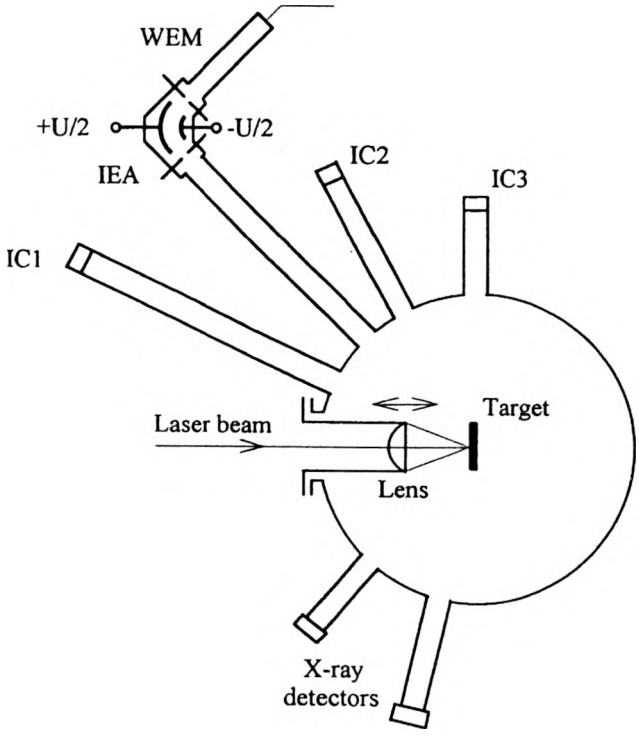


Fig. 1. Scheme of experimental setup and arrangement of diagnostic systems with an aspherical lens illumination system.

Investigations of heavy ion emission from laser-produced plasma were also performed by a team from the IPPLM in joint experiments (*e.g.*, [3]–[5]) at the Institute of Physics ASCR in Prague, with the use of iodine laser PERUN ($E_L < 40$ J, $\tau_L = 350-700$ ps, $I_L > 10^{15}$ Wcm$^{-2}$, $\lambda_L = 1.315$ μm and 2nd as well as 3rd harmonics) and employing the same diagnostic apparatus.

In our experiments we used ion collectors (IC), a cylindrical electrostatic ion energy analyzer (IEA) and a Thomson parabola mass-spectrograph (TP). Both the collectors and electrostatic ion energy analyzer utilize the time-of-flight method

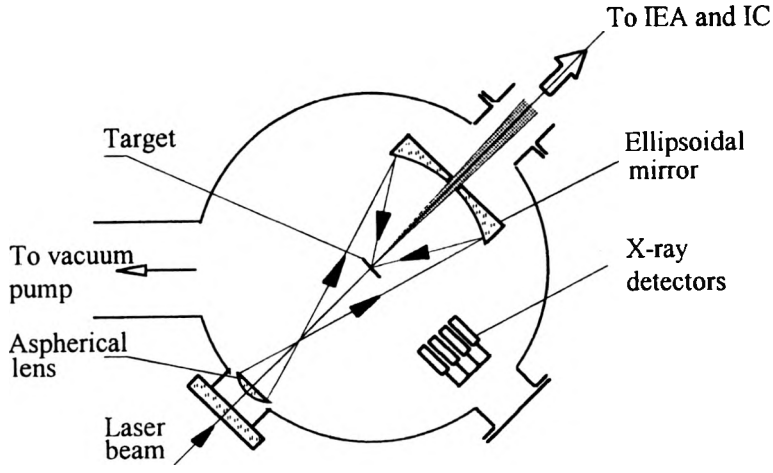


Fig. 2. Scheme of experimental setup and arrangement of diagnostic systems with an aspherical lens – ellipsoidal mirror illumination system.

(TOF). In the TP, ions are analysed by static electric and magnetic fields parallel to each other and perpendicular to the ion stream [9]. The IC measures a charge -integrated time-resolved signal of ions, from which the energy-charge product and the total charge carried by ions, as well as the mean ion energy can be derived [10]. The shape of this signal together with its amplitude give also an indication about the operating conditions (focus setting, laser stability). If a realistic value of the secondary ion-electron emission coefficient of the detector material is available, the ion current density and the corresponding number of ions can be calculated from the IEA and IC signals.

The IEA gives the possibility to identify the ion species produced, *i.e.*, to determine their mass-to-charge ratios, energies and abundance [10]. A windowless electron multiplier (WEM) was used as an ion detector behind the IEA. Calibration of WEMs was performed with the use of the CRYEBIS ion source at the Kansas State University [8]. For high-Z targets the ion species identification as well as the determination of ion energy distributions is a very time-consuming process because it is necessary to evaluate a large number of IEA spectra with several tens of peaks for different deflection potentials. In addition, the peaks of the contaminating ions (especially C and O) are mixed with the ion peaks of interest. To make the evaluation of the experimental spectra easier and to help further data processing, a computer program was developed [9].

The Thomson parabola spectrograph is capable of registering the velocity distribution of all the ion species in a single laser shot [9], [10]. Although the TP has a low energetic dynamic range and a low mass resolution for energetic and highly charged heavy ions, it can provide useful and quick information on ion species and the underlying physical processes in the plasma. However, it is an excellent device for an analysis of the contaminants and low-Z plasma studies.

## 4. Estimation of the principal plasma parameters

In the case of the IEA, the formula combining the measured voltage amplitude of ions $U_z(t)$ for a given charge state $z$ and the current of ions reaching the WEM of the IEA $i_z$ (into the solid angle of the input slit of the IEA) is [10]

$$i_z(t) = ez\left(\frac{dN_z}{dt}\right) = \frac{U_z(t)}{R_l \delta G_e(z,t)} \tag{2}$$

where $R_l$ is the load resistance, $\delta \simeq 10^{-2}$ is the transmittance of the IEA, $G_e$ – the current gain of the WEM, and $t$ – the time of flight of ions. Using very simple formulas: $dN_z/dv_i = (dN_z/dt)(dt/dv_i)$ and $dN_z/dE_i = (dN_z/dv_i)(dv_i/dE_i)$, where $v_i$ is the ion velocity, we can obtain the velocity or energy distribution of each ion species existing in the plasma.

By integration of any of the distributions, the total number of ions of various charge states $N_z$ was calculated. Using these values, the total number of ions, the average charge state of the plasma and abundance of ion species were determined. The ion current $i_{IC}$ or the time derivative of the ion charge $dQ/dt$ at the entrance aperture for a given moment of time $t$ is

$$i_{IC} = \frac{dQ}{dt} = \frac{U_{IC}}{\varepsilon R_{load}[1+\bar{\gamma}(t)/\bar{z}(t)]} \tag{3}$$

where: $U_{IC}$ is the voltage amplitude of the collector signal, $\varepsilon$ the transparency of the entrance mesh, $\bar{\gamma}$ and $\bar{z}$ are the average secondary ion-electron emission coefficient and average charge state of ions. For absolute measurements of the Ta ion flux characteristics the influence of secondary electron emission effect on the IC signal was estimated in [11].

From Equation (3) the velocity $dQ/dv_i$ and energy distributions $dQ/dE_i$ of the ion charge can be obtained; and by integrating them it is possible to calculate the total charge (or the total number of ions) and the total energy carried by the ions as well as the mean ion energy $\bar{E}_i$.

Taking into account the average charge state of ions $\bar{z}$ from the IEA measurements and the mean ion energy of plasma from the ion collector measurements, one can estimate the electron temperature $T_{e,0}$ and the average charge state $\bar{z}_0$ in the region of interaction of laser radiation with the plasma. The electron temperature $T_{e,0}$ of plasma was determined from relation between mean ion energy $\bar{E}_i$, the temperature $T_{e,0}$ and the mean ion charge state $\bar{z}_0$ of plasma [12], [13]

$$\bar{E}_i = C(\bar{z}_0+1)T_{e,0} \tag{4}$$

where: $C = 3.33-5$ is a constant depending on the model of plasma expansion used (*e.g.*, for isothermal expansion $C = 4$). The mean ion energy $\bar{E}_i$ was found from relation

$$\bar{E}_i = \frac{\int (dQ/dE_i)E_i dE_i}{\int (dQ/dE_i)dE_i} \tag{5}$$

where: $dQ/dE_i = d(N_i e\bar{z})/dE_i$ is the distribution of ion charge as a function of ion energy, which was obtained from transformation of ion current pulses measured by the ion collector. The mean ion charge $\bar{z}_0$ in the hot region of plasma was calculated with the use of the formula [14], [15]

$$\bar{z}_0 = K_z \sqrt{\frac{T_e(\text{keV})}{1+\frac{K_z^2}{Z^2}T_e(\text{keV})}} \tag{6}$$

where: $Z$ is the atomic number of the target material, $K_z$ – the constant dependent on the kind of target material. Values of constant $K_z$ for selected target materials are: 35 for C, 37 for $SiO_2$, 40 for Al, 45 for Cu, 47 for Ta and 50 for Au [15].

Following the model of isothermal expansion of plasma, one can sufficiently accurately describe the ion velocity distribution by an exponential relation [16]–[18]

$$\frac{d(N_i e\bar{z})}{dv_i} \sim \exp\left(-\frac{v_i}{c_T}\right) \tag{7}$$

where: $N_i e\bar{z}$ is the total ion charge, $c_T = (\bar{z}_0 T_{e,0}/m_i)^{1/2}$ is the ion sound velocity corresponding to the electron temperature $T_{e,0}$. The slope of ion velocity distribution plot determines the ion sound velocity $c_T$.

A typical ion spectrum from the IEA, and the charge collector signal are presented in Fig. 3. The energy distributions of Ta ion species, shown in Fig. 4, were obtained on the basis of about 50 laser shots in a wide range of deflection plate voltages of the IEA. The abundance of ion species of Ta plasma are presented in Fig. 5. The secondary ion-electron emission coefficient was not taken into account during Ta data treatment. Similar investigations were performed for the other targets.

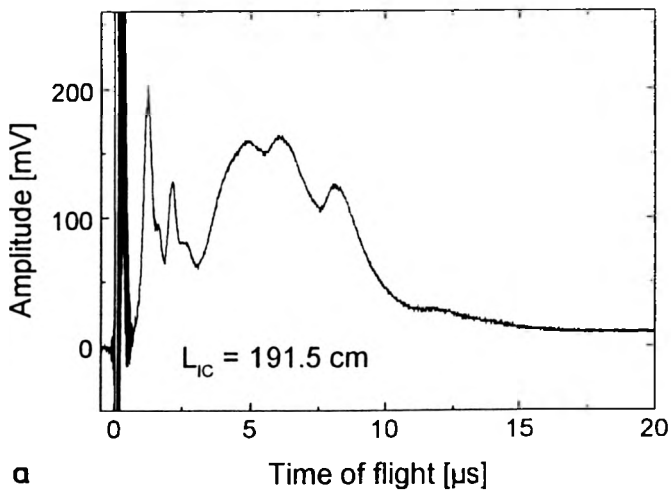


a

Fig. 3a

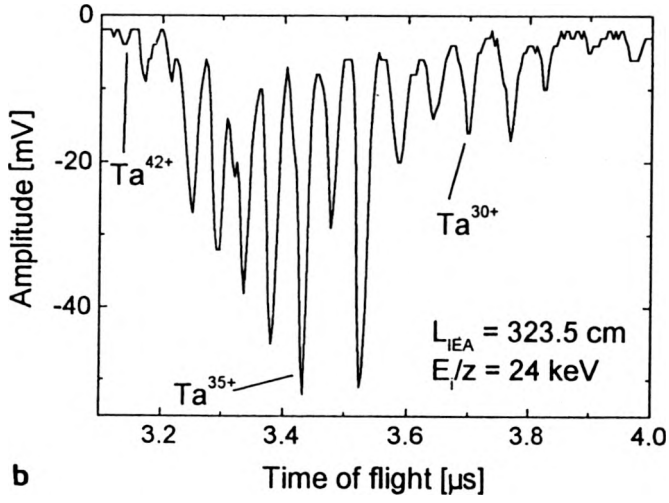


Fig. 3b

Fig. 3. Typical charge-integrated time-resolved signal of Ta ions registered with ion collector (**a**) and time-dependent signal of Ta ions measured with ion energy analyzer (**b**).

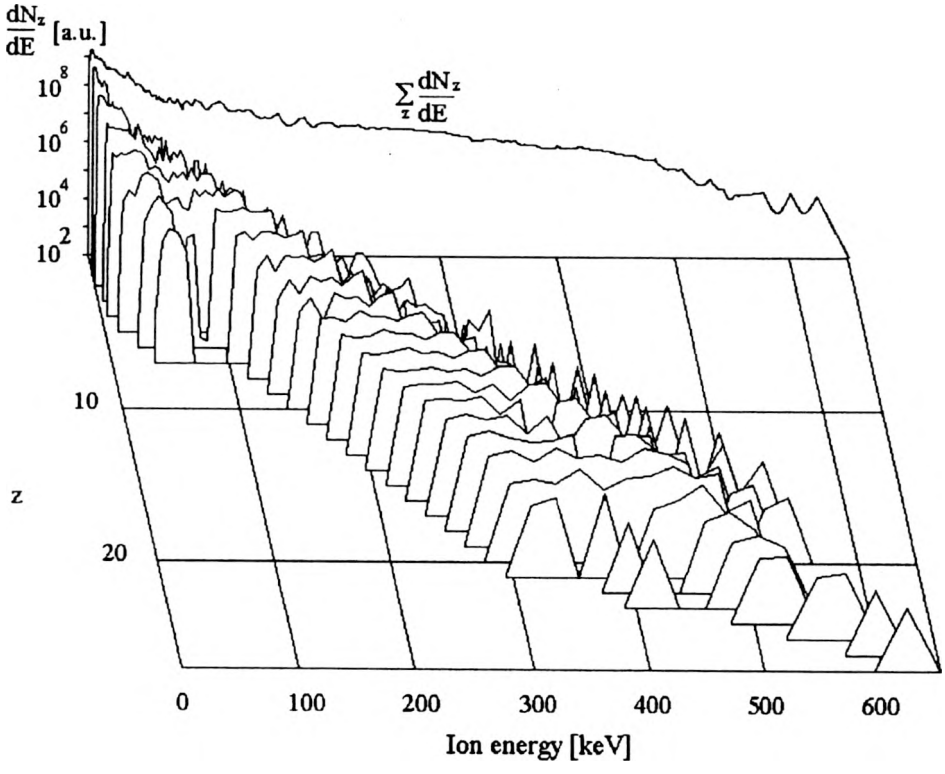


Fig. 4. Energy distribution of Ta ions species estimated on the basis of the IEA signals measured at different deflecting potentials (different $E_i/z$ ratios).

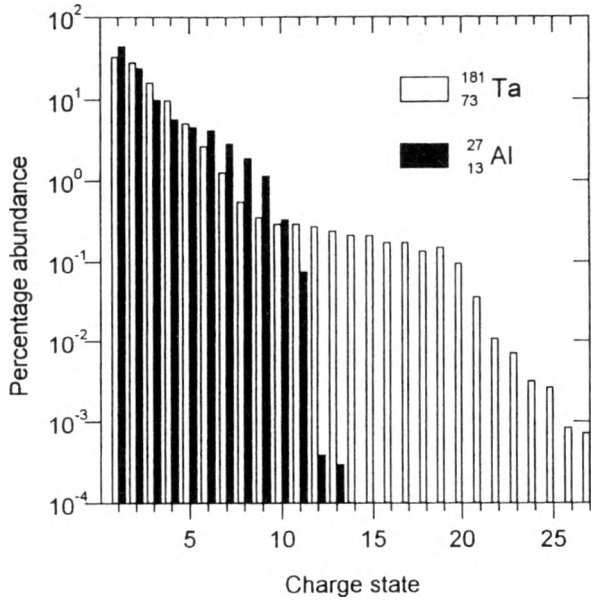


Fig. 5. Percentage abundance of Al and Ta ions determined by integration of energy distributions of ions with a given charge state.

From the equation of Thomson parabola (*e.g.* [9], [10])

$$x = A \frac{m_i U_{el}}{zB^2} y^2 \tag{8}$$

where: $A$ is a constant for a given spectrometer, $U_{el}$ — the potential difference between the electrostatic plates, $B$ — the magnetic field. It is inferred that ions of identical $m_i/z$ ratios are arranged in the same parabola. A fixed $x$ corresponds to a fixed ratio $E_i/z$ = const. and points of different parabolas lying on the vertical line ($y$ = const.) have the same ratios $m_i v_i/z$. The processing of the experimental results is very similar to that described for the IEA, and leads to the preparation of ion energy distributions for each ionization state of registered ions $dN_z/dE_i$ as well as other ion flux parameters.

The ion yield depends strongly on the focusing conditions. The optimum focus setting is defined as the focus position corresponding to the maximum ion current from IC and to the highest charge state from the IEA. It was determined that in the conditions occurring in the experimental setup presented in Fig. 1 the best focal position of the laser beam, for Ta and Pb targets, was about 0.5 mm inside the target surface.

The angular distribution of ions is one of the important characteristics of laser-produced plasma. Its knowledge helps to explain some aspects of plasma expansion and physical processes taking place in the plasma (the relation to laser light absorption, the mechanism of ion acceleration, *etc.*). Measurements of angular distributions of ion emission make it also possible to obtain quantitative data on the total charge, the energy carried out by ions and so on.

## 5. Emission of fast ions

IC signals usually show more than one group of ions (Fig. 3a), the existence of which corresponds to the different mechanisms of their generation. Depending on the experimental condition either fast ions or slow ions were registered beside the group of thermal ions. The mechanism of production of the ions slower than thermal ions is discussed in Sec. 6. The thermal ion group consists of low charge state ions. The faster ion group in the collector signal, if analysed by the IEA is found to be composed of the high charge state of ions and of light contamination ions (H, C and O).

Under the optimum focusing conditions, in the experiments performed at the IPPLM with Nd:glass laser, the maximum charge state obtained was $z_{max} = 42$ and the maximum kinetic ion energy $E_{max} \approx 1$ MeV for Ta plasma, while $z_{max} = 34$ and $E_{max} \approx 1.1$ MeV for Pb plasma.

With the use of the iodine laser [4]–[6], during the joint experiments at IP ASCR in Prague, the electron temperature $T_{e,0} \approx 1.75$ keV and the maximum charge state $z_{max} \sim 55$ for Ta ions were estimated. We registered ions with energies about 9 MeV at power densities higher than $10^{15}$ Wcm$^{-2}$. The maximum total ion current density was 32.4 mAcm$^{-2}$ for Co ions and 35.3 mAcm$^{-2}$ for Ta ions (at a distance of 100 cm). The angular distributions of total charge density are peaked close to the target normal for all the focus settings with respect to the target surface.

From Thomson parabolas obtained for high-Z plasma it can be seen that expanded ion streams are composed of a few groups with different charge states and different velocities [19]–[21]. The fastest group of ions with the charge states $z > 40$ has energies $E_i > 3$ MeV.

Fast ion generation was also investigated in $CO_2$ laser-produced plasma with $I_L < 5 \cdot 10^{11}$ Wcm$^{-2}$ ($E_L = 10-100$ J, $\tau_L \simeq 80$ ns) in experiments performed at IPPLM. The ion energy spectra of different charge states were measured by an ion energy electrostatic analyzer. Two or three groups of ions were encountered. They differed in energy to charge state ratio for thermal ions $E_i/z \leqslant 3$ keV; for the first group of fast ions $3 \leqslant E_i/z \leqslant 10$ keV; and for the second group of fast ions $E_i/z > 10$ keV. The dependence of the average kinetic energy on the charge states of both thermal and fast ions is linear as shown in Fig. 6. The fast ion energy cannot be explained by the adiabatic expansion of plasma at temperatures lower than 500 eV (measured by X-ray and ion diagnostics).

The analysis and calculations of the influence of various phenomena on the generation of hot electrons in the plasma produced by $CO_2$ showed that the Langmuir turbulence of parametric instabilities origin, together with acceleration in the resonant field, can lead to generation of electrons of temperature $T_{e,h} \leqslant 2$ keV. The occurrence of such electrons was confirmed by the detection of X-rays and ion measurements [2]. Electrons of temperature $T_{e,h} > 10$ keV can be generated by accelerating the electrons of the Maxwellian tail in the resonant field, while the electron passes through the field.

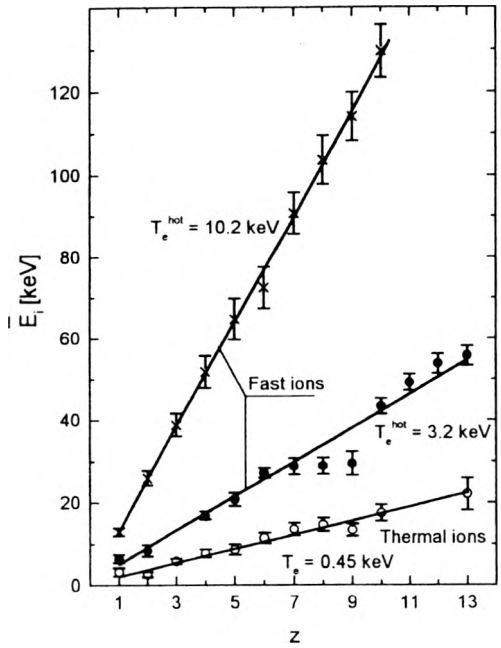


Fig. 6. Mean energy of thermal and two groups of fast Al ions emitted from $CO_2$ laser-produced plasma as a function of ion charge state.

In the laser plasma the non-classical absorption gives birth to a population of suprathermal hot electrons. As a result, at least two groups of ions (thermal and fast) are emitted from the plasma. The ions are gaining their energy during the heating stage of the plasma formation (isothermal expansion), which is followed by a large scale adiabatic expansion into the vacuum. The charge of the escaping ions is determined by ionisation processes in the hot plasma and a subsequent three-body recombination during the adiabatic expansion – the so-called charge freezing. Consequently, according to the conventional hydrodynamic theory (*e.g.*, [17], [22]), the highly charged ions produced by a sub-nanosecond laser pulse should not occur in the far expansion zone. These predictions, however, do not agree with our experiments. A possible way of explaining the occurrence of high charge state ions in the far expansion zone is offered by the existence of the fast ion group seen on the collector signals, which always contains the high charge states. The existence of the fast group means that the plasma time evolution follows the mechanism of two-temperature isothermal expansion [18]. During the expansion phase, first the hot electrons leave the plasma pulling the ions behind. The thermal electrons follow, guiding the thermal group of ions. To support this concept a series of model calculations were performed assuming that the laser energy deposition process renders a two-temperature electron energy distribution possible, which, in turn, leads to a two-temperature exponential density profile. Simulated collector signals and ion charge state distribution calculated on the basis of this simplified model are in a good agreement with the experimental results [23].

## 6. Non-ideal high-Z laser-produced plasma

The properties of plasma are controlled by both the hydrodynamical parameters and the Coulomb type interaction of charged particles in plasma. A plasma can be called ideal if the Coulomb coupling energy is negligible compared with the kinetic energy of particles in the plasma. The measure of discrepancy from the ideality is accepted to be the coupling constant of plasma thought as the ratio of the mean interaction energy of neighbouring particles to their mean kinetic energy [24]. The coupling constant of an ideal plasma is much less than one. A plasma with the coupling constant greater than one is referred to as non-ideal or strongly coupled plasma.

Using the results of ion measurements we have determined relations $E_i^{tot} = f(Z)$, $N_i = f(Z)$, $\bar{E} = f(Z)$, and $T_{e,0} = f(Z)$, where: $E_i^{tot}$ and $N_i$ are the energy carried by ions and the number of ions, respectively, emitted in 1 sr solid angle. For target material of $Z > 13$, two groups of ions have been registered: ions emitted from laser-heated plasma and ions from cooler plasma produced by radiation generated in the laser-heated plasma [2], [25]. With an increase of $Z$ for ions in the cooler plasma $N_i$ and $\bar{E}_i$ (Fig. 7) as well as $E_i^{tot}$ [25] increase rapidly but $T_{e,0}$ is approximately constant for both groups of ions [26]. For Ta and Au targets $N_i$ for ions from cooler plasma is over 10 times higher than $N_i$ for ions from hot plasma (Fig. 7**a**). This ratio for $\bar{E}_i$ (Fig. 7**b**) is about 0.1, for $E_i^{tot}$ exceeds two, whereas for $T_{e,0}$ is about 0.2 [25].

Taking the obtained values of $T_{e,0}$ and $\bar{z}_0$ from formulas (4) and (6) and assuming a solid state ion density $n_i$ we have determined the plasma coupling constant as a ratio of Coulomb energy to kinetic energy in plasma [24]. For Cu, Ta and Au plasma heated by X-rays we have obtained: 8.2, 10.5 and 11.8, respectively, which means that here exists strongly coupled non-ideal plasma. For thermal plasma we have obtained coupling constants: 0.09, 0.14 and 0.14 for Cu, Ta and Au, respectively.

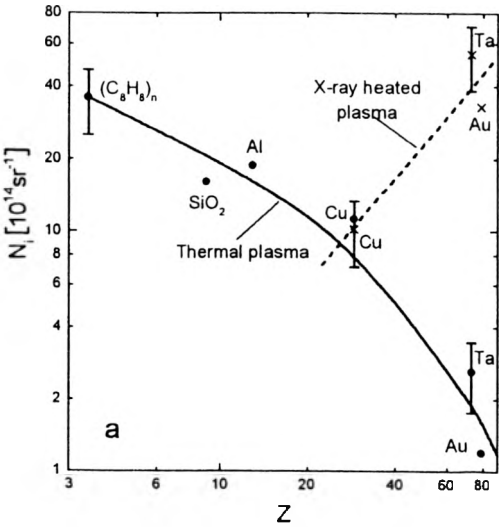


Fig. 7**a**

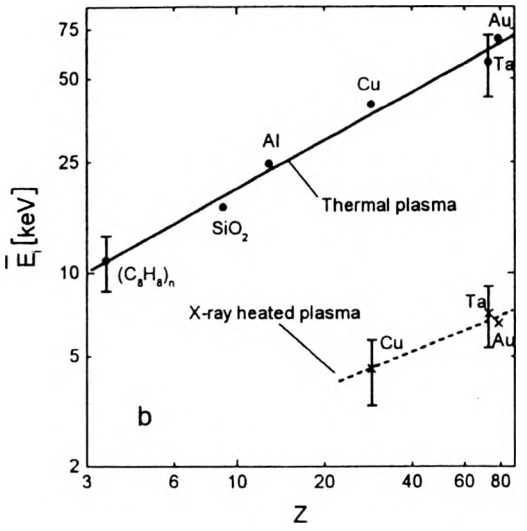


Fig. 7b

Fig. 7. Number of ions (a) and mean ion energy (b) as a function of target $Z$ number for thermal plasma heated directly by laser and plasma hated indirectly by X-rays emitted from thermal plasma.

## 7. Conclusions

The work presents the results of investigations of the properties of the laser -produced plasma of various atomic $Z$ number elements obtained from the measurements of parameters of ion fluxes emitted from the plasma.

The experimental results obtained by the short pulse Nd:glass laser system at the IPPLM and iodine laser system at the IP ASCR provide favourable conditions for the generation of a large amount of ions in high charge states. The complicated processes of the plasma heating generate thermal background plasma and also produce energetic electrons. The energy of these hot electrons is transferred to the fast ions. The fast ions are blown off of the surface of the plasma, which is caused by the hot electrons creating the second peak on the ion collector signal.

A common feature of the ion diagnostics is the fact that they give information about the plasma parameters at a long distance from the target. But from ion measurements, with the use of a proper model of plasma expansion, parameters of plasma at the laser focus spot may be deduced. In spite of this fact, such ion parameters like ion energy distribution, the total number of ions, their average and maximum charge states, the abundance of ion species and energy carried by them give information about mechanisms of the laser interaction with plasma, the absorbed energy, the electron temperature of plasma, *etc.*

On the collector signal generally several maxima can be identified, indicating the existence of several ion groups. Among these fast ions driven by hot electrons, thermal ions and slow ions emitted from secondary focus heated by X-rays and hot electrons from the primary focus are usually recorded.

Anomalous mechanism of radiation absorption in plasma plays an important role in the absorption of the $CO_2$ laser beam even at power density $\leqslant 5 \cdot 10^{11}$ $Wcm^{-2}$. The energy of this radiation is partly transformed into hot electron energy of "temperature" $T_{e,h} \simeq 5\ T_{e,0}$ as a result of resonant absorption and parametric absorption. Groups of fast ions were recorded with $E_i \sim z$ (Fig. 6). These ions can be accelerated in the potential produced by hot electrons.

Short wavelength ($< 1.315$ μm) and short pulse length ($< 1$ ns) lasers are appropriate for generation of the high current of high charge ion streams emitted from laser-produced plasma. This plasma can serve as an effective source of ions for particle accelerators or for ion implantation (*e.g.*, [26]–[28]).

## References


[1] Wołowski J., Plasma Phys. Control. Nuclear Fusion Res. **3** (1985), 163.

[2] Wołowski J., Nowak-Goroszczenko A., Mróz W., Woryna E., Proc. XXI ICPIG, Bohum, Germany, 1993, Vol. II. p. 286.

[3] Parys P., Wołowski J., Woryna E., Farny J., Mróz W., Proc. 23rd ECLIM, Oxford 1994, Inst. Phys., Conf. Ser. No. 104, p. 375.

[4] Woryna E., Parys P., Wołowski J., Láska L., Krása J., Mašek K., Pfeifer M., Krárliková B., Skála J., Straka P., Rohlena K., Appl. Phys. Lett. **69** (1996), 1547.

[5] Rohlena K., Králiková B., Krása J., Láska L., Mašek K., Mocek T., Pfeifer M., Skála J., Straka P., Farny J., Parys P., Wołowski J., Woryna E., Mróz W., Golubev A., Sharkov B., Shumshurov A., Collier J., Haseroth H., Langbein K., Proc. BEAMS'96 Conf., Prague, Czech Republic, 1996, [Ed.] J. Jungwirth, J. Ullschmied, Vol. I, p. 271.

[6] Láska L., Krása J., Mašek K., Pfeifer M., Rohlena K., Králiková B., Skála J., Straka P., Woryna E., Parys P., Wołowski J., Mróz W., Haseroth H., Golubev A., Sharkov B., Korschinek G., Rev. Sci. Instrum. **69** (1998), 1072.

[7] Morse R.L., Nielsen D.W., Phys. Fluids **20** (1973), 909.

[8] Badziak J., Brzeziński R., Gogolewski P., Kuśnierz M., Makowski J., Marczak J., Patron Z., Szczurek M., Ulinowicz A., Proc. 21st ECLIM, Warsaw, Poland, 1991, pp. 131–133.

[9] Mróz W., Pfeifer M., Láska L., Parys P., Woryna E., Proc. 24th ECLIM, Madrid, Spain, June 3–7, 1996, p. 71.

[10] Woryna E., Parys P., Wołowski J., Mróz W., Laser Part. Beams **14** (1996), 293.

[11] Woryna E., Parys P., Wołowski J., Krása J., Láska L., Rohlena K., Stockli M. P., Winecki S., Wlach B., Rev. Sci. Instrum. **69** (1998), 1045.

[12] Tonon G., Rabenau M., J. Plasma Phys. **15** (1973), 871.

[13] Fabbro R., Max C., Fabre E., Phys. Fluids **28** (1985), 1463.

[14] Shearer J.W., Barnes S., Proc. Intern. Conf. LIRPP, Vol. I (1972), 307.

[15] Farny J., Woryna E., Proc. 18th ECLIM, Prague, Czechoslovakia, May 4–8, 1987, p. 85.

[16] Wicknes L.M., Allen J.E., Rumsby P.T., Phys. Rev. Lett. **41** (1978), 249.

[17] Gurevich A.V., Pariskay L.V., Pitaevskii L.P., Sov. Phys. JETP **22** (1975), 449.

[18] Wicknes L.M., Allen J.E., J. Plasma Phys. **22** (1979), 167.

[19] Mróz W., Pfeifer M., Láska L., Woryna E., Proc. 13th Intern. Conf. LIRPP, Monterey, USA, 1996, [Ed.] G.H. Miley, E.M. Campbell, AIP, 1997, p. 621.

[20] Krása J., Láska L., Mašek K., Pfeifer M., Králiková B., Skála J., Straka P., Rohlena K., Mróz W., Woryna E., Parys P., Wołowski J., Haseroth H., Golubev A.A., Sharkov B.Yu., Laser Part. Beams **16** (1998), 5.

[21] Mróz W., Láska L., Krása J., Králiková B., Mašek K., Mocek T., Pfeifer M., Rohlena K., Skála J., Parys P., Wołowski J., Woryna E., Fry D., Stockli P., Rev. Sci. Instrum. **69** (1998), 1349.

[22] Crow J.E., Auer P.L., Allen J.E., J. Plasma Phys. **14** (1975), 65.

[23] WOŁOWSKI J., FARNY J., LÁSKA L., MÄSEK K., PARYS P., ROHLENA K., WORYNA E., Proc. Intern. Conf. LIRPP, Monterey, USA, April 13–18, 1997, pp. 519–526.
[24] ICHIMARU S., Rev. Modern Phys. **54** (1982), 1017.
[25] NOWAK–GOROSZCZENKO A., MRÓZ W., WOŁOWSKI J., WORYNA E., *Physics of Nonideal Plasmas*, Täubner-Texte zur Physik, Stuttgart–Leipzig, 1992, p. 303.
[26] MÄSEK K., KRÁSA J., LÁSKA L., PFEIFER M., ROHLENA K., KRÁLIKOVÁ B., SKÁLA J., WORYNA E., FARNY J., PARYS P., WOŁOWSKI J., MRÓZ W., HASEROTH H., SHARKOV B. YU., KORSCHINEK G., Proc. SPIE **3343** (1999), 254.
[27] WORYNA E., KRÁSA J., LÁSKA L., MÄSEK K., PARYS P., ROHLENA K., WOŁOWSKI J., Proc. XXIV ICPIG, Warsaw 1999, J. Tech. Phys. (in print).
[28] WOŁOWSKI J., PARYS P., WORYNA E., KRÁSA J., LÁSKA L., ROHLENA K., GAMMINO S., CIAVOLA TORRISI L. G., BODDY F. P., HÖPFL R., HORA H., HASEROTH H., Opt. Appl. **30** (2000), 69.

*Received December 3, 1999*
*in revised form February 28, 2000*